Bioconjugate Chemistry

pubs.acs.org/bc

Article

# Palladium-Mediated *S*-Arylation of Cysteine Residues with 4-[$^{18}$F]Fluoroiodobenzene ([$^{18}$F]FIB)

Felix Francis, Melinda Wuest, Jenilee D. Woodfield, and Frank Wuest*

Cite This: *Bioconjugate Chem.* 2024, 35, 232−244

Read Online

ACCESS | Metrics & More | Article Recommendations | Supporting Information

**ABSTRACT:** Transition-metal-mediated bioconjugation chemistry has been used extensively to design and synthesize molecular probes to visualize, characterize, and quantify biological processes within intact living organisms at the cellular and subcellular levels. We demonstrate the development and validation of chemoselective [$^{18}$F]fluoro-arylation chemistry of cysteine residues using Pd-mediated *S*-arylation chemistry with 4-[$^{18}$F]fluoroiodobenzene ([$^{18}$F]FIB) as an aryl electrophile. The novel bioconjugation technique proceeded in excellent radiochemical yields of 73−96% within 15 min under ambient and aqueous reaction mixture conditions, representing a versatile novel tool for decorating peptides and peptidomimetics with short-lived positron emitter $^{18}$F. The chemoselective *S*-arylation of several peptides and peptidomimetics containing multiple reactive functional groups confirmed the versatility and functional group compatibility. The synthesis and radiolabeling of a novel prostate-specific membrane antigen (PSMA) binding radioligand [$^{18}$F]**6** was accomplished using the novel labeling protocol. The validation of radioligand [$^{18}$F]**6** in a preclinical prostate cancer model with PET resulted in favorable accumulation and retention in PSMA-expressing LNCaP tumors. At the same time, a significantly lower salivary gland uptake was observed compared to clinical PSMA radioligand [$^{18}$F]PSMA-1007. This finding coincides with ongoing discussions about the molecular basis of the off-target accumulation of PSMA radioligands currently used for clinical imaging and therapy of prostate cancer.

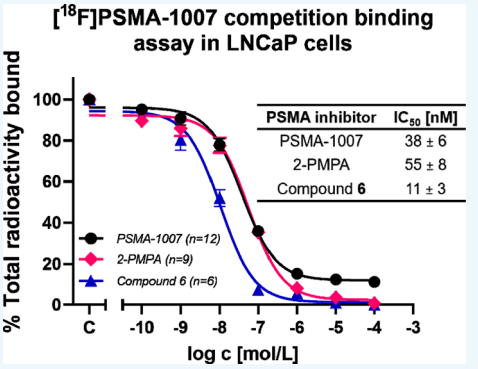




## INTRODUCTION

Transition-metal-mediated bioconjugation chemistry for the chemoselective modification of biomolecules has evolved as a powerful research tool at the crossroads of chemistry and biology, especially for site-selective protein modifications and chemical protein synthesis and manipulation.[1−4] Transition-metal-mediated bioconjugation chemistry has also been used extensively to design and synthesize molecular probes to visualize, characterize, and quantify biological processes within intact living organisms at the cellular and subcellular levels. The complex structure of biomolecules and the diversity of reactive functional groups in biomolecules such as acids, alcohols, thiols, and amines represent particular challenges for developing fast and chemoselective bioconjugation chemistry methods, which proceed under mild reaction conditions.

Cysteine represents an ideal amino acid residue for the chemical modification of peptides and proteins owing to the unique reactivity of thiol groups and the relatively low abundance of cysteine in naturally occurring proteins, enabling high levels of chemo- and regioselectivity of cysteine residues in the presence of other amino acid chains.[5,6] Michael addition chemistry to maleimides and $S_N2$ reactions with alkyl halides are commonly used to conjugate fluorescent dyes, radionuclides, affinity labels, and drug molecules to peptides and proteins to cysteine residues.[3] However, the resulting conjugates tend to decompose in the presence of external bases or other thiol nucleophiles. In this line, cysteine arylation chemistry has been introduced to improve the stability of the cysteine-modified conjugates. Several transition-metal-mediated cysteine arylation reactions have emerged in the past two decades as complementary approaches to $S_NAr$ chemistry with arylation reagents containing strong electron-withdrawing groups, significantly expanding the scope of chemoselective *S*-arylation bioconjugations with peptides and proteins.[1,3,4] Starting with the pioneering work by Buchwald and Pentelute, several Au(III)-, Pd(II)-, and Ni(II)-mediated cysteine arylations have grown extensively during recent years to enable chemoselective arylation of cysteine residues under ambient aqueous reaction mixture conditions.[1,3,4,7,8] The recent success of transition-metal-mediated *S*-arylation bioconjugation chemistry was also applied to small molecules and peptides using $^{18}$F-labeled (hetero)aryl halides to design and synthesize radioligands for positron emission tomography (PET). Humpert et al. reported the radiolabeling of thiol-

**Received:** December 1, 2023
**Revised:** December 23, 2023
**Accepted:** December 28, 2023
**Published:** January 12, 2024




https://doi.org/10.1021/acs.bioconjchem.3c00522
*Bioconjugate Chem.* 2024, 35, 232−244

Table 1. *S*-Arylation of GSH with [$^{18}$F]FIB Using Xantphos Pd G3

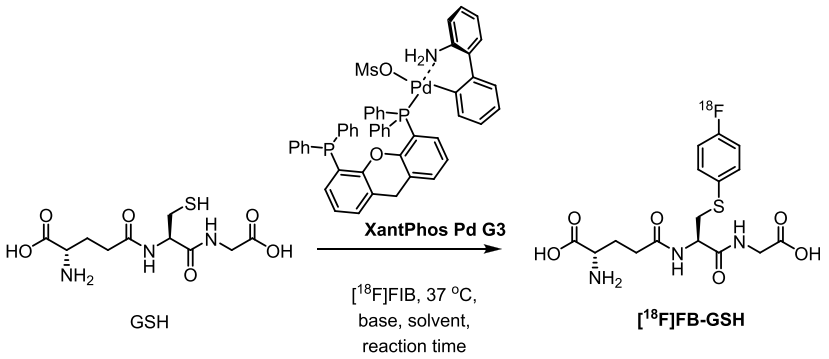


| entry | GSH($\mu$mol) | XantPhos Pd G3(mol %) | base (equiv) | solvent | time (min) | RCY[a] (%) |
|---|---|---|---|---|---|---|
| 1 | 10 | 1 | $NEt_3$ (1) | THF/$H_2O$ (1:1) | 30 | 73 ± 4 ($n$ = 6) |
| 2 | 10 | 1 | $NEt_3$ (1) | $CH_3CN$/$H_2O$ (1:1) | 30 | 69 ± 2 ($n$ = 3) |
| 3 | 10 | 1 | DBU (1) | THF/$H_2O$ (1:1) | 30 | 17 ± 6 ($n$ = 3) |
| 4 | 10 | 1 | no base | THF/$H_2O$ (1:1) | 30 | 29 ± 2 ($n$ = 2) |
| 5 | 3 | 1 | $NEt_3$ (1) | THF/$H_2O$ (1:1) | 15 | 71 ± 3 ($n$ = 3) |
| 6 | 3 | 1 | $NEt_3$ (3) | THF/$H_2O$ (1:1) | 30 | 80 ± 3 ($n$ = 3) |
| 7 | 0.3 | 1 | $NEt_3$ (3) | THF/$H_2O$ (1:1) | 30 | 83 ± 1 ($n$ = 9) |
| 8 | 1 | 10 | $NEt_3$ (3) | THF/$H_2O$ (1:1) | 15 | 91 ± 1 ($n$ = 6) |
| 9 | 0.3 | 10 | $NEt_3$ (3) | THF/PBS (1:1) | 15 | 96 ± 3 ($n$ = 10) |
| 10 | 0.3 | 10 | $NEt_3$ (3) | $CH_3CN$/PBS (1:1) | 15 | 94 ± 5 ($n$ = 14) |

[a]Radiochemical yields (RCYs) were determined by radio-HPLC, representing the percentage of product present in the reaction mixture.

containing compounds via Pd-mediated *S*-arylation with 2-[$^{18}$F]fluoro-5-iodopyridine. The rapid radiofluorination process proceeded in an aqueous medium, and the preparation of $^{18}$F-labeled glutathione, a PSMA radioligand, an oligomer-binding RD2 peptide, and bovine serum albumin in radiochemical yields ranging from 10 to 55% demonstrated the feasibility of the proposed *S*-arylation chemistry with 2-[$^{18}$F]fluoro-5-iodopyridine.[9]

More recently, McDaniel et al. described the rapid radiofluorination via *S*-arylation chemistry of unprotected peptides and sugars in aqueous media with an organometallic Au(III)-[$^{18}$F]fluoroaryl complex. The *S*-arylation protocol using 4-[$^{18}$F]fluoroiodobenzene ([$^{18}$F]FIB) as an aryl electrophile was applied to several thiol-containing peptides and sugars with excellent radiochemical yields in the 70−95% range.[10]

Over the last two decades, our research team and others have extensively used [$^{18}$F]FIB as a versatile radiolabled electrophile in several Pd-mediated C−C and C−N cross-coupling reactions employing Stille, Suzuki−Miyaura, Sonogashira, and Hartwig−Buchwald *N*-arylation chemistry for the synthesis and modification of structurally diverse $^{18}$F-labeled compounds, including steroids, nucleosides, COX-2 inhibitors, $\sigma_2$ inhibitors, biphenyls, amino acids, $AT_1$ antagonists, D4 ligands, statins, and peptides.[11−14] Despite the need for individual optimization of reaction conditions, the described Pd-mediated cross-coupling reactions proved to be a valuable synthesis tool to significantly expand the arsenal of $^{18}$F-labeled compounds, in addition to recent groundbreaking advancements and developments in late-stage and electrophilic radiofluorination chemistry.[15−17] The compatibility toward a wide range of functional groups, the versatility to form distinct C−C and C−N bonds in a given molecule, and the mild reaction conditions of Pd-mediated cross-couplings with [$^{18}$F]FIB have made this class of reactions a popular and efficient radiolabeling strategy with short-lived positron emitter fluorine-18 ($^{18}$F, $t_{1/2}$ = 109.8 min).

The present study describes the development of a versatile and site-specific radiofluorination strategy of peptides and peptidomimetics using innovative Pd-mediated *S*-arylation chemistry with [$^{18}$F]FIB as a readily available aryl electrophile for chemoselective modification of cysteine residues. We have recently developed a fully automated [$^{18}$F]FIB synthesis enabling the preparation of large amounts (4−6 GBq) of [$^{18}$F]FIB in high radiochemical and chemical purity starting from commercially available (4-iodophenyl)diphenylsulfonium triflate as the labeling precursor.[11,18] The first part of our work deals with optimizing reaction conditions for Pd-mediated *S*-arylation chemistry with [$^{18}$F]FIB using cysteine-containing tripeptide glutathione (GSH). Then, we tested the chemoselectivity and functional group compatibility of *S*-arylation chemistry with model peptides LCKLSL and LYCWHL, representing typical amino acid residues in peptides and proteins. Finally, we prepared and studied novel $^{18}$F-labeled prostate-specific antigen (PSMA) radioligand [$^{18}$F]FB-Cys-urea-Glu ([**$^{18}$F**]**6**) using optimized Pd-mediated *S*-arylation chemistry conditions. Radiopharmacology of novel PSMA radioligand [**$^{18}$F**]**6** was tested *in vitro* and *in vivo* in comparison with clinically used radiotracers [$^{18}$F]DCFPyL and [$^{18}$F]PSMA-1007, including cellular uptake and PET studies in PSMA-expressing LNCaP prostate cancer cells.

## RESULTS

**Optimization of *S*-Arylation Chemistry with Glutathione (GSH).** 4-[$^{18}$F]Fluoro-iodobenzene ([$^{18}$F]FIB) was synthesized in 78 ± 11% decay-corrected radiochemical yield after HPLC purification via our reported automated procedure using a sulfonium salt precursor.[18] [$^{18}$F]FIB prepared from sulfonium or iodonium salt precursors for transition-metal-mediated cross-coupling reactions must be purified by HPLC


https://doi.org/10.1021/acs.bioconjchem.3c00522
Bioconjugate Chem. 2024, 35, 232−244

**Scheme 1. Structure of *S*-Arylated Model Peptides [$^{18}$F]FB-LCKLSL and [$^{18}$F]FB-LYCWHL**

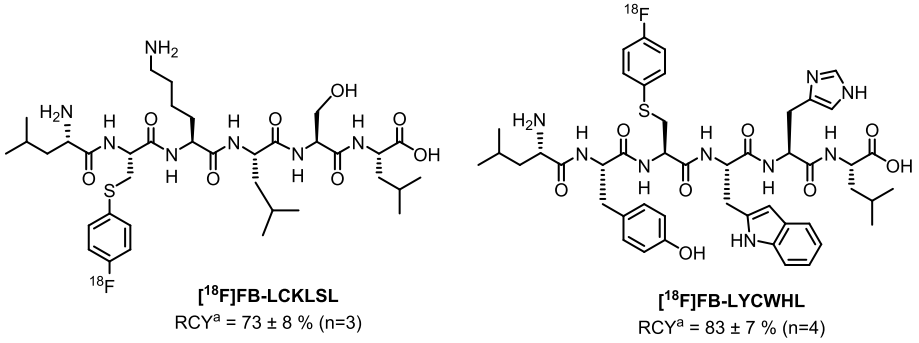


[a]Radiochemical yields (RCYs) were determined by radio-HPLC, representing the percentage of product present in the reaction mixture.

**Scheme 2. Synthesis of Labeling Precursor 5 and Reference Compound 6**

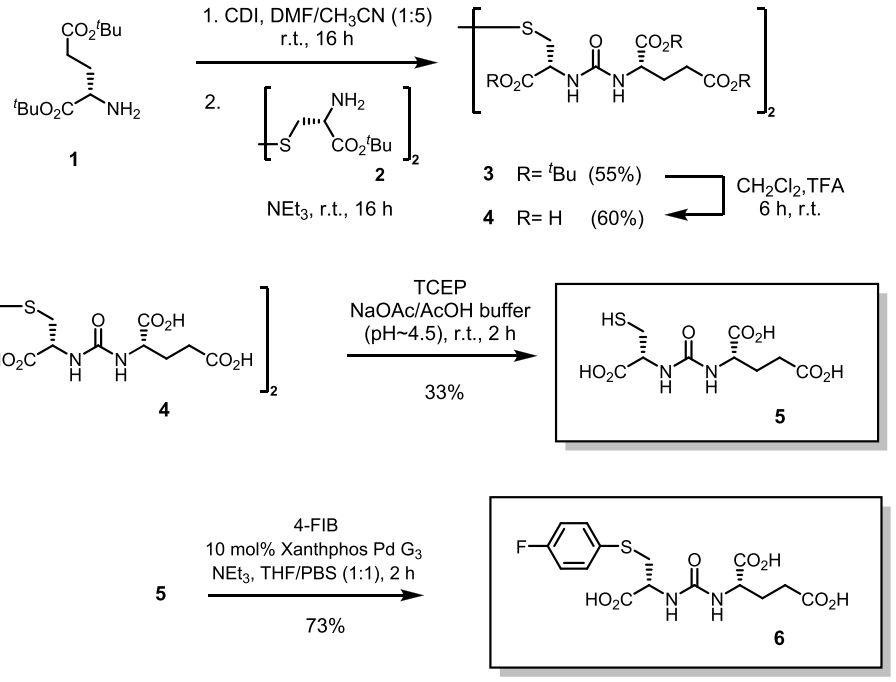


to remove aryl iodide side products providing [$^{18}$F]FIB in high radiochemical and chemical purity exceeding 95%. HPLC-purified [$^{18}$F]FIB was used to screen reactions with cysteine-containing tripeptide L-glutathione (GSH) to optimize Pd-mediated *S*-arylation reaction conditions. We selected XantPhos Pd G3 as an excellent transition metal complex for Pd-mediated cross-coupling reactions, including functionalizing peptides containing cysteine residues. XantPhos Pd G3 is a third-generation (G3) Buchwald precatalyst based on a 2-aminobiphenyl scaffold. It is air, moisture, and thermally stable and is highly soluble in a wide range of common organic solvents. Unique properties and features of XantPhos Pd G3 include lower catalyst loadings, shorter reaction times, efficient formation of the active catalytic species, and accurate control of ligand-to-palladium ratio.[19]

Initial test reactions with 10 $\mu$mol (~3 mg) GSH, Pd G3 XantPhos (1 mol %), $NEt_3$ (1 equiv) in 50% aqueous THF or $CH_3CN$ at 37 °C afforded desired *S*-arylated product [$^{18}$F]FB-GSH in promising 73 ± 4% and 69 ± 4% radiochemical yield, respectively, within 30 min (entries 1 and 2). 15−20 MBq of [$^{18}$F]FIB was used in all reactions summarized in Table 1. Changing the solvent mixture to combinations other than 50% aqueous $CH_3CN$ or THF seemed to impact the reaction negatively (data not shown); hence, only 50% aqueous mixtures of THF or $CH_3CN$ were further considered for the screening reactions. Changing the base from $NEt_3$ to 1,8-diazabicyclo[5.4.0]undec-7-ene (DBU) or removing a base from the reaction mixture led to lower radiochemical yields of 17−21% (entries 3 and 4). Lowering the peptide amount to 3 $\mu$mol (~0.9 mg) still gave [$^{18}$F]FB-GSH in good radiochemical yields of 71 ± 3% within 15 min (entry 5). Increasing the amount of $NEt_3$ from 1 equiv (entry 1) to 3 equiv while lowering the amount of GSH to 3 $\mu$mol (~0.9 mg) and 0.3 $\mu$mol (~0.09 mg) resulted in an even higher radio-chemical yield of 80−83% (entries 6 and 7). However, a further increase of the base amount to 10 equiv had a detrimental effect on the homogeneity of the reaction mixture, resulting in lower radiochemical yields (data not shown). Using 10 mol % of the Pd-complex increased the radiochemical yield to a reproducible >90% in the presence of low GSH amounts (1 $\mu$mol (~0.3 mg) and 0.3 $\mu$mol (~0.09 mg)) within 15 min in


https://doi.org/10.1021/acs.bioconjchem.3c00522
Bioconjugate Chem. 2024, 35, 232−244

Scheme 3. Automated Radiosynthesis of PSMA Radioligand [$^{18}$F]6

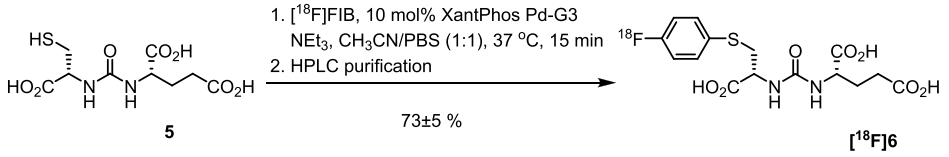


THF/$H_2O$ and THF/PBS (entries 8 and 9). A comparable result was observed with $CH_3CN$/PBS as a solvent (entry 10).

However, using GSH amounts <0.3 $\mu$mol led to inconsistent results. Table 1 summarizes the optimization of reaction conditions for Pd-mediated *S*-arylation with [$^{18}$F]FIB using GSH.

Optimized reaction conditions with cysteine-containing tripeptide GSH include the reaction of 0.3 $\mu$mol (~0.09 mg) GSH, XantPhos Pd G3 (10 mol %), $NEt_3$ (3 equiv) in 50% aqueous (PBS)/THF or $CH_3CN$ at 37 °C affording *S*-arylated product [$^{18}$F]FB-GSH in excellent and reproducible radiochemical yields of 94−96% within 15 min. Moreover, the identity of *S*-arylated product [$^{18}$F]FB-GSH was confirmed by radio-HPLC analysis and comparing retention times with respective reference compound FB-GSH.

**Chemoselectivity and Functional Group Compatibility Testing with Model Peptides.** Optimized reaction conditions for the *S*-arylation were applied to model peptides to assess the chemical scope of the methodology regarding functional group compatibility and chemoselectivity. The chemoselectivity of the Pd-mediated *S*-arylation protocol with [$^{18}$F]FIB was tested with hexapeptides LCKLSL and LYCWHL containing amino acid residues for potential *N*- and *O*-arylation side reactions. However, *S*-arylated peptides [$^{18}$F]FB-LCKLSL and [$^{18}$F]LYCWHL were obtained in high radiochemical yields of 73−83%, and the formation of respective *N*- or *O*-arylated products was not observed (Scheme 1).

Model hexapeptide LCKLSL contains reactive primary amine (K) and alcohol groups (S) in addition to the N- and C-terminus. The chemoselective *S*-arylation reaction of LCKLSL with [$^{18}$F]FIB was successful using optimized reaction conditions summarized in Table 1 (entry 9), providing radiopeptide [$^{18}$F]FB-LCKLSL in 73 ± 8% radiochemical yield.

Hexapeptide LYCWHL containing phenol (Y), indole (W), and imidazole (H) groups was also tested for chemoselective *S*-arylation with [$^{18}$F]FIB using optimized reaction conditions. Radiopeptide [$^{18}$F]FB-LYCWHL was obtained in 83 ± 7% radiochemical yield.

The chemoselectivity and functional group compatibility of the *S*-arylation protocol toward cysteine in the presence of other amino acid residues were further confirmed by analyzing radiolabeled peptides [$^{18}$F]FB-LCKLSL and [$^{18}$F]FB-LYCWHL with radio-HPLC and comparing retention times with respective reference compounds.

**Chemical Synthesis of PSMA Ligand 6 and Labeling Precursor 5.** The synthesis of novel cysteine-containing PSMA ligand FB-Cys-urea-Glu **6** and respective labeling precursor Cys-urea-Glu **5** is shown in Scheme 2.

The synthesis commenced with our recently reported 1,1′-carbonyl-diimidazole (CDI)-mediated one-pot urea synthesis protocol[20] starting from di-*tert*-butyl glutamate **1** and di-*tert*-butyl cystine **2** to generate the desired Cys-urea-Glu dimer **3** in 55% yield. Disulfide **3** was treated with trifluoroacetic acid for *tert*-butyl ester deprotection, which proceeded in 60% yield to give compound **4**.

Reduction of the disulfide bond in **4** was achieved with tris(2-carboxyethyl)phosphine (TCEP), affording labeling precursor **5** in 33% yield. Compound **5** was subjected to *S*-arylation reaction conditions with 4-FIB in the presence of Xantphos Pd G3 to obtain reference compound **6** in 73% yield.

**Radiochemistry.** Following the success of the *S*-arylation chemistry with [$^{18}$F]FIB using cycteine-containing peptides GSH, LCKLSL, and LYCWHL, we expanded the optimized synthesis procedure to peptidomimetics by preparing novel PSMA radioligand [$^{18}$F]FB-Cys-urea-Glu [$^{18}$**F**]**6**. Labeling precursor **5** was subjected to optimized *S*-arylation reaction conditions to afford radioligand [$^{18}$**F**]**6** in good radiochemical yields of 73 ± 5% starting from [$^{18}$F]FIB (Scheme 3). We also performed the radiosynthesis in an automated synthesis unit (ASU), which afforded radioligand [$^{18}$**F**]**6** in good isolated radiochemical yields (decay-corrected) of 21 ± 6% starting from cyclotron-produced [$^{18}$F]fluoride and a radiochemical purity exceeding 95% after HPLC purification. The molar activity was ~40 GBq/$\mu$mol, and the total synthesis time was 120 min, including HPLC purification and preparation of an injectable formulation suitable for subsequent *in vitro* and *in vivo* studies.

**Lipophilicity.** According to literature protocols, the octanol−water distribution coefficient (log *D*) of PSMA radioligand [$^{18}$**F**]**6** was determined by the shake-flask method using *n*-octanol and PBS at pH 7.4.[21] The log *D* at pH 7.4 for radioligand [$^{18}$**F**]**6** was −2.7, pointing to the hydrophilic nature of the radioligand.

***In Vitro* Binding Assay.** Compound **6** was tested for its PSMA inhibitory potency in an *in vitro* competitive binding assay using PSMA-expressing prostate cancer cell line LNCaP and [$^{18}$F]PSMA-1007 as the PSMA-binding radioligand.

2-(Phosphonomethyl)-pentanedionic acid (2-PMPA) and PSMA-1007, both known high-affinity PSMA inhibitors, were used as positive controls and reference compounds. Compound **6** displayed a low nanomolar $IC_{50}$ value of 11 ± 3 nM, confirming high-affinity binding to PSMA suitable for cellular uptake and inhibition studies in LNCaP cells as well as *in vivo* evaluation of radioligand [$^{18}$**F**]**6** using PET in an LNCaP xenograft model.

Compound **6** exhibited similar inhibitory potency as PSMA inhibitor 2-(3-(1-carboxy-5-[(6-fluoro-pyridine-3-carbonyl)-amino]-pentyl)-ureido)-pentanedioic acid (DCFPyL, $IC_{50}$ = 13 nM)[22] and a higher inhibitory potency than positive controls PSMA-1007 (38 ± 6 nM) and 2-PMPA (55 ± 8 nM) used in the binding assay. The result of the *in vitro* competition assay in LNCaP cells is summarized in Figure 1.

**Cellular Uptake and Inhibition Studies in LNCaP Cells.** Cellular uptake and blocking studies of radioligand **6** in LNCaP are shown in Figure 2.

Uptake of radioligand [$^{18}$**F**]**6** was studied in the prostate cancer cell line LNCaP. The highest uptake of radioligand [$^{18}$**F**]**6** was observed at 90 min, reaching 7.9 ± 0.8%


https://doi.org/10.1021/acs.bioconjchem.3c00522
Bioconjugate Chem. 2024, 35, 232−244

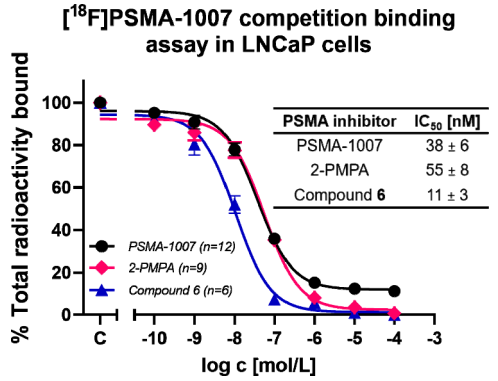


**Figure 1.** PSMA binding of compound **6** was determined in LNCaP cells using [$^{18}$F]PSMA-1007 as the radioligand and PSMA-1007 and 2-PMPA as positive controls. C represents normalized total radioactivity bound to LNCaP cells (100%) without the inhibitor. Data are shown as mean ± SEM from *n* experiments.

radioactivity/mg protein. The uptake of radioligand [$^{18}$F]**6** did not further increase for the remaining time of the study. PSMA specificity of radioligand uptake in LNCaP cells was further tested with cellular uptake inhibition studies using high-affinity PSMA inhibitor DCFPyL and compound **6**. LNCaP cells were preincubated with 0.1, 1.0, and 1000 $\mu$M DCFPyL and 1 mM compound **6** for 30 min before adding radioligand [$^{18}$F]**6**. Radioligand uptake could be reduced in a concentration-dependent manner using DCFPyL, resulting in a 40, 66, and 77% blocking effect, respectively. Self-blocking with compound **6** at 1 mM resulted in a 71% blocking effect.

**PET in LNCaP Tumor-Bearing Mice.** PSMA targeting properties of radioligand [$^{18}$F]**6** were tested in LNCaP tumor-bearing mice and compared to the clinically used radioligand [$^{18}$F]PSMA-1007. Representative images displayed as the maximum-intensity projection (MIP) at 60 min postinjection (p.i.) of 6−8 MBq of radioligands [$^{18}$F]PSMA-1007 and [$^{18}$F]**6** and respective time-activity curves of the tumor and muscle uptake under control and [$^{18}$F]**6** tumor uptake under blocking conditions with DCFPyL and compound **6** are shown in Figure 3.

The radioligand [$^{18}$F]**6** accumulates and retains in tumor tissue with an $SUV_{60\ min}$ of 1.03 ± 0.2 ($n$ = 5) while displaying low muscle uptake and retention, resulting in an $SUV_{60\ min}$ of 0.17 ± 0.05. Radioligand [$^{18}$F]**6** was cleared primarily through the kidneys. Additional radioactivity uptake and retention were detected in the liver and spleen. Radioligand [$^{18}$F]PSMA1007 showed high tumor uptake and retention ($SUV_{60\ min}$ 2.19 ± 0.42) and similar low muscle uptake and retention ($SUV_{60\ min}$ 0.26 ± 0.05) as radioligand [$^{18}$F]**6**. PSMA-mediated tumor uptake of radioligand [$^{18}$F]**6** was confirmed with blocking experiments using PSMA inhibitors DCFPyL and compound **6** for self-blocking.

Blocking experiments in the same mice with DCFPyL (300 $\mu$g) and compound **6** (300 $\mu$g) demonstrated that tumor uptake of radioligand [$^{18}$F]**6** was significantly reduced by 75% ($SUV_{60\ min}$ 0.24 ± 0.02) and 60% ($SUV_{60\ min}$ 0.4 ± 0.01), respectively. Interestingly, the radioactivity uptake and retention in the salivary glands was significantly lower for radioligand [$^{18}$F]**6** compared to [$^{18}$F]PSMA1007, reaching a $SUV_{60\ min}$ 0.21 ± 0.06 (radioligand [$^{18}$F]**6**) and $SUV_{60\ min}$ 1.08 ± 0.15 ([$^{18}$F]PSMA1007) (Figure 4).

## DISCUSSION

Over the last decades, advances in transition-mediated cross-coupling chemistry have stimulated the development of novel bioconjugation methods for the chemo- and regioselective modification of peptides and proteins. The presence of many different functional groups in peptides and proteins represents a formidable challenge for chemo- and regioselective modifications. In this line, Pd-mediated chemistry has evolved as a powerful tool, allowing highly efficient and selective biochemistry reactions under mild conditions compatible with peptides and proteins' delicate structural and functional integrity. Among the diverse functional groups present in peptides and proteins, the unique reactivity of the thiol group and its importance in chemical synthesis and chemical biology make cysteine residues particularly valuable for chemoselective bioconjugations using Pd-mediated *S*-arylation chemistry. *S*-arylation chemistry led to the synthesis of several macrocyclic peptides, covalent protein modulators, and antibody−drug conjugates.[3,4] The method was also used to functionalize unprotected peptides with various chemical entities, including fluorescent tags, affinity labels, bioconjugation handles, and photochemical cross-linkers. However, only a few reports described transition metal-mediated *S*-arylation chemistry to prepare $^{18}$F-labeled radioligands for PET using organometallic Au(III) and Pd(II) complexes.[9,10]

The present study focused on developing and validating a novel chemoselective bioconjugation method of cysteine residues using Pd-mediated *S*-arylation chemistry with readily

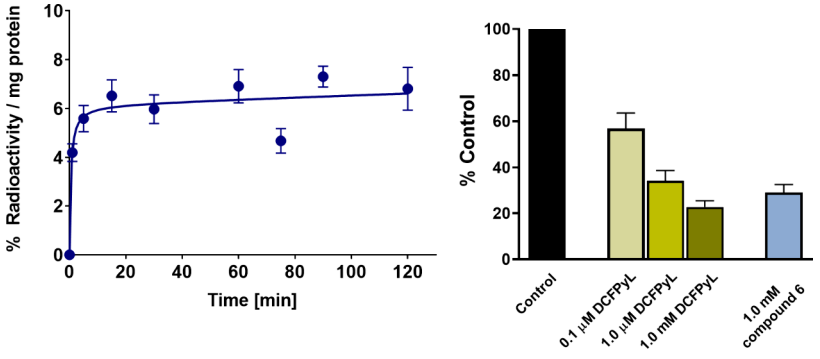


**Figure 2.** Uptake of radioligand [$^{18}$F]**6** into LNCaP cells over 120 min. Data are normalized as % radioactivity per mg protein and shown as mean ± SEM from $n$ = 3 experiments (left). Blocking of radioligand [$^{18}$F]**6** uptake (60 min incubation time) into LNCaP cells using different concentrations of high-affinity PSMA inhibitor DCFPyL and high concentration (1.0 mM) of compound 6. Data are normalized as % maximum uptake of radioligand [$^{18}$F]**6** and analyzed as mean ± SEM from $n$ = 3 experiments (right).


https://doi.org/10.1021/acs.bioconjchem.3c00522
Bioconjugate Chem. 2024, 35, 232−244

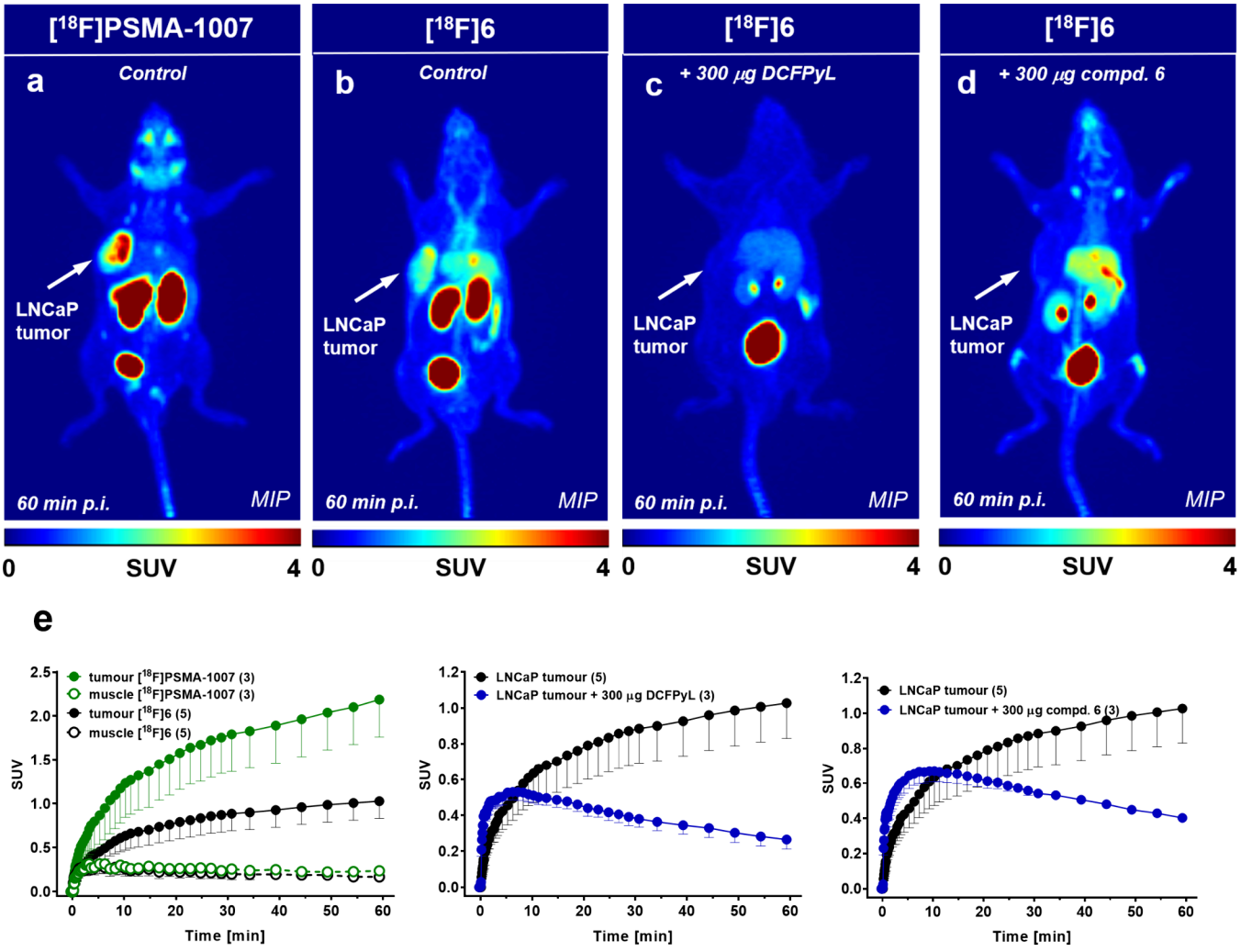


**Figure 3.** Representative images (maximum intensity projection) of LNCaP tumor-bearing mice 60 min after injection of radioligands [$^{18}$F]PSMA-1007 (a) and [$^{18}$F]**6** (b) in the absence and the presence of 300 $\mu$g of DCFPyL (c) and compound **6** (d). Corresponding time-activity curves show radioactivity profiles in LNCaP tumors under both conditions compared to muscle tissue as mean ± SEM from $n$ = 5 (control) and $n$ = 3 (blocked experiments) (e).

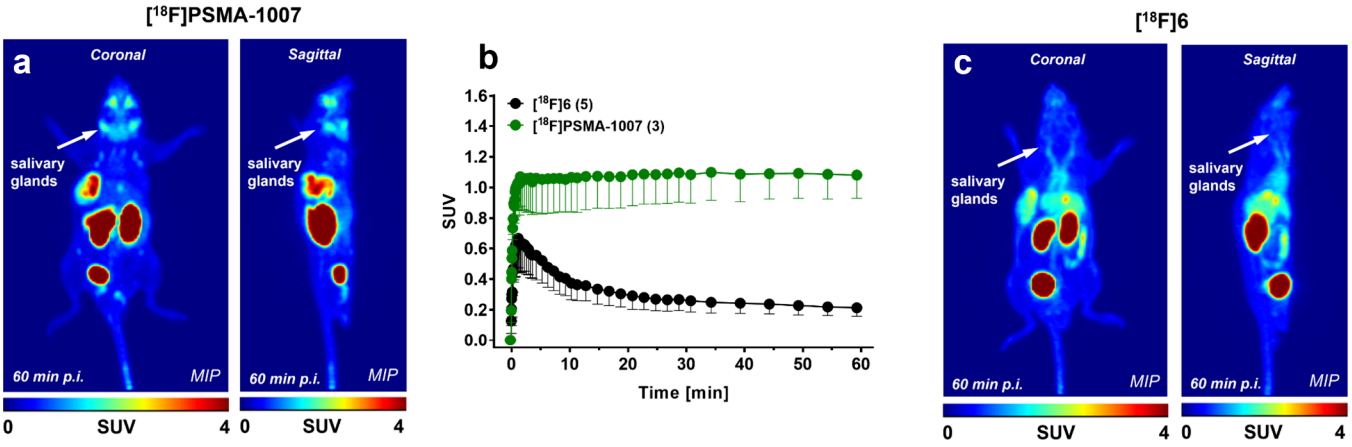


**Figure 4.** Representative images (maximum intensity projection) of salivary glands in LNCaP tumor-bearing mice 60 min after injection of radioligands [$^{18}$F]PSMA-1007 (a) and [$^{18}$F]**6** (c). Corresponding time−activity curves (b) show radioactivity profiles in salivary glands of both radioligands as mean ± SEM from $n$ = 5 ([$^{18}$F]**6**) and $n$ = 3 ([$^{18}$F]PSMA-1007).

available $^{18}$F building block [$^{18}$F]FIB as an electrophile. The availability of phosphine-ligated Pd complexes is critical to the success of Pd-mediated coupling reactions for generating carbon−carbon and carbon-heteroatom bonds, including *S*-arylation chemistry with [$^{18}$F]FIB. Over the last two decades, several generations of Pd complexes containing phosphine


https://doi.org/10.1021/acs.bioconjchem.3c00522
Bioconjugate Chem. 2024, 35, 232−244

ligands have been developed and tested in C−C and C-heteroatom cross-coupling reactions.[3,7,19] Typical examples comprise Pd(II) complexes containing phosphine ligands *XPhos*, *BrettPhos*, and *XantPhos*. Third-generation Pd complex XantPhos Pd G3 based on a 2-aminobiphenyl scaffold (Table 1) can be easily activated under mild conditions to generate the desired ligand-Pd(0) species to enter the catalytic cycle.[19] Moreover, the reported air, moisture, thermal stability, and high solubility in a wide range of solvents make complex XantPhos Pd G3 an ideal choice for the proposed Pd-mediated *S*-arylation of peptides with [$^{18}$F]FIB. Reaction conditions were screened and optimized with tripeptide L-glutathione (GSH) as a model peptide testing different solvents, reaction times, and amounts of GSH and XantPhos Pd G3 (Table 1).

Optimized ambient and aqueous reaction mixture conditions afforded *S*-arylated product [$^{18}$F]FB-GSH in 94−96% radiochemical yield, representing the product percentage in the reaction mixture. The identity of [$^{18}$F]FB-GSH was determined by radio-HPLC analysis via coinjection with reference compound FB-GSH.

Observed radiochemical yields of 94−96% for *S*-arylation of GSH are comparable with reported radiochemical yields using Au(III) and XantPhos Pd G3 in the presence of and [$^{18}$F]FIB and 5-iodo-2[$^{18}$F]fluoropyridine as aryl electrophiles, respectively.[9,10] However, optimized reaction conditions allowed using as little as 0.3 $\mu$mol (0.09 mg) of GSH compared to the reported 3.0 and 16 $\mu$mol of GSH, making our protocol particularly suitable for the radiolabeling of biomolecules like peptides and proteins with $^{18}$F at low concentrations.

The demonstrated chemoselectivity and functional group compatibility of Pd-mediated *S*-arylation chemistry with [$^{18}$F]FIB using model peptides LCKLSL and LYCWHL further highlight the suitability of the novel bioconjugation protocol for the rapid and efficient incorporation of $^{18}$F into peptides. The possibility to perform the reaction under ambient and aqueous reaction mixture conditions in the presence of unprotected amino acid residues represents a significant advantage, which also warrants the testing of the novel $^{18}$F bioconjugation method to other thiol-containing biomolecules such as small proteins and antibody fragments. However, the proposed *S*-arylation chemistry has limitations and challenges, such as the required two-step synthesis protocol involving preparing and purifying [$^{18}$F]FIB as an aryl electrophile before the cross-coupling reaction. The introduction of a [$^{18}$F]fluoroaryl motif also leads to a lipophilicity increase of the radioligand, which can be considered an additional challenge when comparing the Pd-mediated *S*-arylation chemistry with [$^{18}$F]FIB with current one-step radiofluorination strategies using [$^{18}$F]AlF-NOTA and isotopic exchange on trifluoroborates.[23]

Nuclear medicine molecular imaging and therapy of prostate cancer have witnessed an unprecedented pace by introducing prostate-specific membrane antigen (PSMA) targeting urea-based peptidomimetics as radioligands. Typical clinical examples comprise [$^{18}$F]PSMA-1007, [$^{18}$F]DCFPyL, [$^{68}$Ga]-PSMA-11, and [$^{177}$Lu]PSMA-617, all containing a Lys-urea-Glu scaffold as the PSMA pharmacophore.[24] However, early attempts to develop urea-based small molecule PSMA radioligands for PET also considered peptidomimetics based on a Cys-urea-Glu backbone.[25] Early radiolabeling of Cys-urea-Glu peptidomimetics with $^{18}$F was accomplished through an *S*-alkylation reaction with 4-[$^{18}$F]fluorobenzyl bromide providing PSMA radioligand *N*-[*N*-[(*S*)-1,3-dicarboxypropyl]-carbamoyl]-4-[$^{18}$F]fluorobenzyl-L-cysteine ([$^{18}$F]DCFBC), which displayed favorable *in vitro* and *in vivo* pharmacokinetics for PET imaging of prostate cancer.[25]

Radioligand [$^{18}$F]DCFBC displayed an $IC_{50}$ value of 13.9 nM and favorable tumor uptake and retention in PSMA-expressing PC-3 PIP tumors.[25] We envisioned peptidomimetic Cys-urea-Glu for radiolabeling with $^{18}$F using Pd-mediated *S*-arylation chemistry with [$^{18}$F]FIB to prepare novel PSMA radioligand [$^{18}$F]FB-Cys-urea-Glu ([$^{18}$F]**6**) as a structural analog of [$^{18}$F]DCFBC.

Application of our recently developed synthesis protocol of urea-based PSMA inhibitors with *N*-alkyl carbamoylimidazoles afforded peptidomimetic Cys-urea-Glu **5** as the labeling precursor.

Novel PSMA radioligand [$^{18}$F]**6** was prepared in average isolated and decay-corrected radiochemical yields of 21%, confirming the versatility and highly flexible nature of the proposed Pd-mediated *S*-arylation chemistry with [$^{18}$F]FIB.

Radioligand [$^{18}$F]**6** shares almost the same structure as radioligand [$^{18}$F]DCFBC, except for lacking a methylene group between the cysteine residue and the aryl motif. The comparable $IC_{50}$ values of radioligand [$^{18}$F]**6** ($IC_{50}$ = 11 nM) and [$^{18}$F]DCFBC ($IC_{50}$ = 13 nM) also reflect the structural similarity of both PSMA inhibitors. Cellular uptake and inhibition studies confirmed PSMA-mediated uptake in PSMA-expressing LNCaP cells, which was also demonstrated in PET imaging experiments using LNCaP xenografts. The observed tumor uptake and retention profile and biodistribution and clearance pattern of radioligand [$^{18}$F]**6** align with published data for radioligand [$^{18}$F]DCFBC, further confirming the structural similarity of both radioligands and the typical biodistribution and elimination profile for urea-based PSMA radioligands. PET with radioligand [$^{18}$F]**6** were compared to the current clinically used radioligand [$^{18}$F]PSMA-1007. Although overall tumor uptake and retention of radioligand [$^{18}$F]**6** was lower than that of [$^{18}$F]PSMA-1007 ($SUV_{60\ min}$ = 1.03 ± 0.2 versus $SUV_{60\ min}$ = 2.19 ± 0.42), radioligand [$^{18}$F]**6** displayed significantly lower uptake and retention in salivary glands as a prominent healthy tissue often showing high PSMA radioligand accumulation. PSMA, also known as glutamate carboxypeptidase II (GCPII), is a clinically validated target highly expressed in prostate cancer lesions. Recently, [$^{177}$Lu]-PSMA-617 (Pluvicto) reached FDA approval as the first radioligand for radiotherapy of progressive, PSMA-positive metastatic castration-resistant prostate cancer (mCRPC).[26] Patients treated with Pluvicto benefited from extended overall survival compared to those treated with the standard of care. Nevertheless, several patients undergoing Pluvicto treatment discontinued treatment due to undesired side effects, including xerostomia (dry mouth). The mechanisms underlying PSMA radioligand accumulation in healthy tissues like salivary glands are not yet fully understood. However, recent reports describe GCPIII as a potential off-target causing the accumulation and retention of clinically used PSMA radioligands [$^{177}$Lu]Lu-PSMA-617 and [$^{18}$F]PSMA-1007 in healthy tissue like salivary glands.[27]

Authors of the study discuss that several Glu-ureido PSMA ligands, like radioligands [$^{177}$Lu]Lu-PSMA-617 and [$^{18}$F]PSMA-1007, display structural similarities to the natural PSMA substrate *N*-acetyl-aspartyl-glutamate (NAAG), leading to cross-reactivity with PSMA (GCPII) and GCPIII.

This hypothesis has prompted the development of PSMA radioligands such as [$^{68}$Ga]Ga-JB-1498 binding selectively to


https://doi.org/10.1021/acs.bioconjchem.3c00522
Bioconjugate Chem. 2024, 35, 232−244

GCPII over GCPIII, which resulted in no or only minimal radioligand uptake in GCPIII expressing healthy tissues like kidneys and salivary glands in a mouse model.[28] Radioligands [$^{18}$F]**6** and [$^{18}$F]DCFBC also showed only minimal uptake in GCPIII-expressing salivary glands, making them potential leads for developing GCPII-selective radioligands.

However, another report claims that GCPIII is not the off-target for urea-based PSMA ligands, demonstrating the controversial nature of the discussion and the lack of detailed knowledge on PSMA (GCPII) and GCPIII pharmacology.[29]

However, recent findings with PSMA radioligand [$^{68}$Ga]Ga-JB-1498 and our novel radioligand [$^{18}$F]**6** points to the need for future research to decipher the mechanistic basis for the accumulation or no accumulation of PSMA radioligands in healthy tissue like kidneys and salivary glands.

## CONCLUSIONS

We have reported the development and validation of a novel bioconjugation method for the chemoselective [$^{18}$F]-fluoroarylation of cysteine residues using Pd-mediated *S*-arylation chemistry with [$^{18}$F]FIB. The novel bioconjugation technique proceeded in good radiochemical yields under ambient and aqueous reaction mixture conditions, representing a versatile novel tool for decorating peptides with short-lived positron emitter $^{18}$F. The rapid kinetics, the mild reaction conditions, the functional group compatibility, and the use of only submicromolar amounts of cysteine-containing labeling precursor add Pd-mediated *S*-arylation chemistry with [$^{18}$F]FIB as a valuable method to the few existing transition metal-mediated bioconjugation techniques of peptides with $^{18}$F and therefore expanding the growing radiochemical space of using transition metals in $^{18}$F chemistry. The possibility of performing the novel bioconjugation method in the presence of unprotected amino acid residues warrants the extension to other thiol-containing biomolecules, including small proteins and antibody fragments. Moreover, the present work also described the synthesis and validation of novel PSMA radioligand [$^{18}$F]**6**, confirming the versatility of the novel Pd-mediated *S*-arylation chemistry with [$^{18}$F]FIB. The validation of radioligand [$^{18}$F]**6** in a preclinical prostate cancer model with PET resulted in favorable accumulation and retention in PSMA-expressing LNCaP tumors. At the same time, a significantly lower salivary gland uptake was observed compared to clinical PSMA radioligand [$^{18}$F]PSMA-1007. This finding coincides with ongoing discussions about the molecular basis of the off-target accumulation of clinical radioligands that are currently used for imaging and therapy. It may stimulate novel developments for synthesizing novel PSMA radioligands with desirable high tumor uptake while showing no or only minimal uptake in healthy tissues such as salivary glands and kidneys.

## EXPERIMENTAL SECTION

**General.** All chemicals, reagents, and solvents for synthesis and analysis were of analytical grade and were used without further purification. HPLC-grade acetonitrile and trifluoroacetic acid were purchased from Sigma-Aldrich. Anhydrous acetonitrile and dimethylformamide were purchased from Acros Organics. All peptide synthesis reagents were purchased from NovaBioChem and used without purification. Peptides were synthesized via automated solid phase peptide synthesis (SPPS) using the Syro I peptide synthesizer (MultiSynTech/Biotage, USA). Reaction parameters were screened using an Eppendorf Thermomixer R and an IKAMAG Ret-G Stir plate with an oil bath. Semipreparative HPLC was performed on a Gilson system with a 321 pump, a photodiode array detector, and a HERM Bertolt radiodetector installed with a Phenomenex Luna 5 $\mu$m polyfluorophenyl (PFP) and Phenomenex Luna 10 $\mu$m C-18 column. UV absorbance was monitored at 210 or 254 nm wavelength. The mobile phase consisted of water/0.2%TFA as solvent A and acetonitrile as solvent B. QMA cartridges were purchased from ABX advanced biochemical compounds GmbH, Strata X cartridges were purchased from Phenomenex and Sep-Pak Silica Plus Long Cartridges were purchased from Waters Corporation. $^{1}$H NMR and $^{13}$C NMR spectra were recorded on an Agilent/Varian Inova two-channel 400 MHz spectrometer, an Agilent/Varian Inova four-channel 500 MHz spectrometer, and an Agilent/Varian VNMRS three-channel 600 MHz spectrometer. Chemical shifts are given in ppm referenced to internal standards (s = singlet, bs = broad singlet, d = doublet, dd = doublet of doublet, ddd = doublet of doublet of doublet, t = triplet, M = multiplet, m = massif). High-resolution mass spectrometry (HR-MS) was carried out on an Agilent Technologies 6220 oaTOF. LC-MS was carried out on an Agilent Technologies 6130 LCMS system.

**Chemical and Peptide Synthesis.** *FB-GSH.* A oven-dried borosilicate reaction vial with septa cap (7 mL) was charged with XantPhos Pd-G$_3$ (10 mg, 0.0108 mmol), reduced glutathione (55 mg, 0.18 mmol), 1-fluoro-4-iodobenzene (120.2 mg, 0.541 mmol), and PBS/THF (1:1, 1.3 mL). This mixture was allowed to stir at room temperature under an argon atmosphere for ∼1 min. After the mixing period, NEt$_3$ (45 mL, 0.541 mmol) was added using a syringe. This mixture was stirred at room temperature for 120 min. After this, the mixture was diluted with 10 mL of CH$_3$CN and was subjected to semipreparative HPLC purification. (3 mL/min, 0−5 min 20% B, 15 min 50% B, 15−20 min 50% B, 25 min 90% B, 25−35 min 90% B.)

The fractions containing the pure product ($t_R$ = 22.5−23.5 min) were combined and lyophilized to obtain FB-GSH as an off-white solid in 84% yield (61 mg, 0.153 mmol). **$^{1}$H NMR** (500 MHz, DMSO-$d_6$) $\delta$ 7.38 (s, 4H), 4.45 (dd, $J$ = 8.8, 4.1 Hz, 1H), 3.72 (d, $J$ = 3.7 Hz, 2H), 3.66 (t, $J$ = 6.1 Hz, 1H), 3.35 (dd, $J$ = 13.5, 4.2 Hz, 1H), 3.06 (dd, $J$ = 13.6, 9.1 Hz, 1H), 2.34 (dd, $J$ = 8.7, 7.2 Hz, 2H), 1.97 (dd, $J$ = 13.3, 6.6 Hz, 2H); **$^{13}$C NMR** (126 MHz, DMSO-$d_6$) $\delta$ 171.74, 171.01, 170.91, 170.37, 134.82, 130.97, 130.60, 129.13, 52.54, 51.93, 41.05, 35.41, 31.18, 26.46. **HR-MS (ESI-TOF):** calcd. for $C_{16}H_{21}FN_3O_5S^-$ $(M-H)^-$ 400.1077; found 400.1019.

*Peptide Synthesis.* Peptides LCKLSL and LYCWHL were synthesized on a fully automated peptide synthesizer (Syro I, Multisyn-tech/Biotage) using Fmoc-orthogonal solid phase peptide synthesis starting from alkoxybenzyl alcohol (Wang) resin with an initial load of 0.6 mmol/g. A detailed description of the synthetic procedure and cleavage conditions can be found in previously published manuscripts.[30,31]

*LCKLSL.* HPLC conditions: Phenomenex Luna C-18. A = 0.2% TFA/H$_2$O, B = CH$_3$CN. Flow rate: 3 mL/min, gradient: 0−5 min 20% B, 15 min 50% B, 15−20 min 50% B, 25 min 90% B, 25−35 min 90% B. The fractions containing pure product ($t_R$ = 27−28 min) were mixed and lyophilized to obtain the purified LCKLSL. HR-MS (ESI-TOF): calcd. $m/z$ for $C_{30}H_{58}N_7O_8S$ $(M+H)^+$ 676.4068; found 676.4060.


https://doi.org/10.1021/acs.bioconjchem.3c00522
Bioconjugate Chem. 2024, 35, 232−244

*LYCWHL*. HPLC conditions: Phenomenex Luna C-18, A = 0.2% TFA/$H_2O$, B = $CH_3CN$. Flow rate: 3 mL/min, gradient: 0−5 min 20% B, 15 min 50% B, 15−20 min 50% B, 25 min 90% B, 25−35 min 90% B. The fractions containing pure product ($t_R$ = 25 min) were mixed and lyophilized to obtain the purified LYCWHL. HR-MS (ESI-TOF): calcd. *m*/*z* for $C_{41}H_{56}N_9O_8S$ $(M+H)^+$ 834.3967; found 834.3960.

*FB-LCKLSL*. A 2 mL Eppendorf LoBind microcentrifuge tube was charged with XantPhos Pd-$G_3$ (10 mg, 0.0108 mmol), LCKLSL (20 mg, 0.03 mmol), 1-fluoro-4-iodobenzene (32 mg, 0.14 mmol), and $H_2O$/THF (8:2, 1 mL). The vial was flushed with nitrogen at room temperature and left to mix on a thermoshaker for ∼1 min. After the mixing period, $NEt_3$ (15 mL, 0.15 mmol) was added using a pipet and flushed with nitrogen. This mixture was stirred at room temperature for 60 min. After this, the mixture was diluted with 10 mL (0.2% TFA/$H_2O$; 1:1) of HPLC eluent and was subjected to semipreparative HPLC purification (Phenomenex Luna C-18, A = 0.2% TFA/$H_2O$, B = $CH_3CN$. Flow rate: 3 mL/min. Gradient: 3 mL/min, 0−5 min 20% B, 15 min 50% B, 15−20 min 50% B, 25 min 90% B, 25−35 min 90% B). $t_R$ = 25 min.

The pure product fractions were lyophilized to obtain peptide FB-LCKLSL as a white solid in 66% yield (16 mg, 0.02 mmol). **HR-MS (ESI-TOF):** calcd. *m*/*z* for $C_{36}H_{61}FN_7O_8S$ $(M+H)^+$ 770.4281; found 770.4281.

*FB-LYCWHL*. A 2 mL Eppendorf LoBind microcentrifuge tube was charged with XantPhos Pd-$G_3$ (10 mg, 0.0108 mmol), LYCWHL (20 mg, 0.02 mmol), 1-fluoro-4-iodobenzene (26 mg, 0.12 mmol), and $H_2O$/THF (8:2, 1 mL). The vial was flushed with nitrogen at room temperature and left to mix on a thermoshaker for ∼1 min. After the mixing period, $NEt_3$ (15 mL, 0.15 mmol) was added using a pipet and flushed with nitrogen. This mixture was stirred at room temperature for 60 min. After this, the mixture was diluted with 10 mL (0.2%TFA/$H_2O$; 1:1) of HPLC eluent and was subjected to semipreparative HPLC purification (Phenomenex Luna C-18, A = 0.2% TFA/$H_2O$, B = $CH_3CN$. Flow rate: 3 mL/min. Gradient: 0−5 min 20% B, 15 min 50% B, 15−20 min 50% B, 25 min 90% B, 25−35 min 90% B). $t_R$ = 32−33 min. The pure product fractions **HR-MS (ESI-TOF):** calcd. *m*/*z* for $C_{47}H_{59}FN_9O_8S$ $(M+H)^+$ 928.4186; found 928.4182.

*Hexa-tert-butyl (3S,7R,12R,16S)-5,14-Dioxo-9,10-dithia-4,6,13,15-tetraazaoctade-cane-1,3,7,12,16,18-hexacarboxylate* ***3***. In a 50 mL glass flask equipped with a stir bar, L-glutamic acid di-*tert*-butyl ester HCl **1** (592 mg, 2.0 mmol) and CDI (360 mg, 2.2 mmol) were dissolved in DMF (1 mL) and $CH_3CN$ (5 mL). The solution was stirred at room temperature until complete conversion of the starting material was observed (∼18 h), L-cystine di-*tert*-butyl ester dihydrochloride **2** (850 mg, 2.0 mmol) and $Et_3N$ (700 μL, 2.50 mmol) were added to the reaction mixture. The solution was stirred for 18 h, and volatiles were removed *in vacuo*. The residue obtained was purified by flash chromatography to give urea **3** as a colorless gel in 55% yield (1.01 g, 1.1 mmol). **$^1$H NMR** (500 MHz, $CDCl_3$) δ 6.12 (s, 2H), 5.88 (d, *J* = 7.4 Hz, 2H), 4.68 (dt, *J* = 7.4, 5.3 Hz, 2H), 4.42 (s, 2H), 3.17 (dd, *J* = 13.8, 5.4 Hz, 2H), 3.05 (dd, *J* = 13.8, 5.3 Hz, 2H), 2.40−2.24 (m, 4H), 2.09 (dddd, *J* = 14.2, 9.5, 6.4, 4.9 Hz, 2H), 1.84 (dtd, *J* = 14.6, 9.2, 6.0 Hz, 2H), 1.49−1.41 (m, 54H). **$^{13}$C NMR** (126 MHz, $CDCl_3$) δ 173.18, 172.22, 169.94, 157.09, 82.57, 82.47, 80.50, 53.52, 53.06, 41.77, 31.62, 28.39, 28.11, 28.05, 28.01. **HR-MS (ESI-TOF):** calcd. for $C_{42}H_{74}N_4NaO_{14}S_2$ $[M + Na]^+$ 945.4535; found: 945.4530.

*(3S,7R,12R,16S)-5,14-Dioxo-9,10-dithia-4,6,13,15-tetraa-zaoctadecane-1,3,7,12,16,18-hexa-carboxylic Acid* ***4***. In a 7 mL glass vial with a PTFE cap, compound **3** (50 mg, 0.054 mmol) was treated with 1 mL of $CH_2Cl_2$/TFA (1:1) at 0 °C and the reaction mixture was allowed to warm up to room temperature over 6 h. Subsequent removal of all volatiles from the reaction mixture and purification with preparative HPLC (Phenomenex Luna C-18, A = 0.2% TFA/$H_2O$, B = $CH_3CN$. Flow rate: 2 mL/min. Gradient: 0−15 min 5% B, 20 min 10% B, 35−45 min 40% B. $t_R$ = 33.5 min) resulted in the isolation of desired compound **4** as a white solid in 60% yield (19 mg, 0.032 mmol). **$^1$H NMR** (500 MHz, DMSO-$d_6$) δ 6.54 (d, *J* = 8.2 Hz, 2H), 6.45 (d, *J* = 8.2 Hz, 2H), 4.38 (td, *J* = 7.3, 4.8 Hz, 2H), 4.11 (td, *J* = 7.6, 4.8 Hz, 2H), 3.11 (dd, *J* = 13.5, 5.1 Hz, 2H), 3.04 (dd, *J* = 13.5, 7.3 Hz, 2H), 2.30−2.16 (m, 4H), 1.97−1.86 (m, 2H), 1.72 (ddd, *J* = 10.8, 8.7, 5.6 Hz, 2H); **$^{13}$C NMR** (126 MHz, DMSO-$d_6$) δ 174.00, 173.68, 172.58, 158.44, 158.13, 156.96, 116.39, 114.09, 52.00, 51.61, 41.06, 29.82, 27.50. **HR-MS (ESI-TOF):** calcd. *m*/*z* for $C_{18}H_{25}N_4O_{14}S_2$ $(M-H)^-$ 585.0814; found 585.0814.

*(((R)-1-Carboxy-2-mercaptoethyl)carbamoyl)-L-glutamic Acid* ***5***. In a 7 mL glass vial with a PTFE cap, disulfide **4** (60 mg, 0.10 mmol) and *tris*(2-carboxyethyl)phosphine hydrochloride (33 mg, 0.11 mmol) were dissolved in 1.5 mL of NaOAc/AcOH buffer (100 mM, pH ∼ 4.5). The reaction was allowed to stir at room temperature for 1 h. The reaction mixture was diluted with 10 mL of DI water and subjected to semipreparative HPLC purification (Phenomenex Luna C-18, A = 0.2% TFA/$H_2O$, B = $CH_3CN$. Flow rate: 2 mL/min. Gradient: 0−15 min 5% B, 20 min 10% B, 35−45 min 40% B. $t_R$ = 26.5 min). After lyophilization, compound **5** was obtained in 33% yield (20 mg, 0.033 mmol) as a white solid (very hygroscopic, occasionally presented as a transparent sticky gel which had to be dissolved in minimum $CH_3CN$ and lyophilized again to obtain the solid). **$^1$H NMR** (500 MHz, DMSO-$d_6$) δ 6.72 (d, *J* = 8.2 Hz, 1H), 6.58 (d, *J* = 8.0 Hz, 1H), 4.50 (dt, *J* = 7.9, 4.9 Hz, 1H), 4.24 (td, *J* = 8.3, 5.2 Hz, 1H), 2.96 (dd, *J* = 8.5, 5.0 Hz, 2H), 2.45−2.32 (m, 2H), 2.30 (t, *J* = 8.4 Hz, 1H), 2.09−2.02 (m, 1H), 1.89−1.81 (m, 1H).**$^{13}$C NMR** (126 MHz, DMSO-$d_6$) δ 174.08, 173.69, 172.26, 156.99, 54.18, 51.68, 29.87, 27.45, 26.72. **HR-MS (ESI-TOF):** calcd. *m*/*z* for $C_9H_{13}N_2O_7S$ $(M-H)^-$ 293.0449; found 293.0450.

*((1-Carboxy-2-((4-fluorophenyl)thio)ethyl)carbamoyl)-L-glutamic Acid* ***6***. An oven-dried borosilicate reaction vial with a septa cap (7 mL) was charged with XantPhos Pd-$G_3$ (10 mg, 0.0108 mmol), compound **5** (30 mg, 0.1 mmol), 1-fluoro-4-iodobenzene (120.2 mg, 0.541 mmol), and ($H_2O$/THF; 1:1, 1 mL). This mixture was allowed to stir at room temperature under an argon atmosphere for ∼1 min. After the mixing period, $NEt_3$ (30 mL, 0.3 mmol) was added using a syringe. This mixture was stirred at room temperature for 30 min. After this, the mixture was diluted with 10 mL (0.2%TFA/$H_2O$; 1:1) of HPLC eluent and was subjected to semipreparative HPLC purification (Phenomenex Luna C-18, A = 0.2% TFA/$H_2O$, B = $CH_3CN$. Flow rate: 2 mL/min. Gradient: 0−15 min 5% B, 20 min 10% B, 35−45 min 40% B. $t_R$ = 30.5 min).

The fractions containing the pure product were lyophilized to obtain the TFA salt of compound **6** as a white solid in 63% yield (24 mg, 0.063 mmol). **$^1$H NMR** (498 MHz, $D_2O$) δ 7.58−7.49 (m, 2H), 7.18−7.10 (m, 2H), 4.41 (dd, *J* = 7.5, 4.4 Hz, 1H), 4.22 (dd, *J* = 8.7, 5.2 Hz, 1H), 3.49 (dd, *J* = 14.5, 4.4 Hz, 1H), 3.33 (dd, *J* = 14.5, 7.5 Hz, 1H), 2.50 (t, *J* = 7.3 Hz,


https://doi.org/10.1021/acs.bioconjchem.3c00522
Bioconjugate Chem. 2024, 35, 232−244

2H), 2.21−2.12 (m, 1H), 2.04−1.92 (m, 1H). **$^{13}$C NMR** (126 MHz, DMSO-$d_6$) $\delta$ 173.77, 172.48, 162.00, 156.92, 134.28, 131.88, 131.82, 116.14, 115.96, 52.26, 51.71, 36.95, 29.99, 27.59. $^{19}$F-NMR (469 MHz, $D_2O$) $\delta$ −75.27 (TFA), −114.60. **HR-MS (ESI-TOF)**: calcd. $m/z$ for $C_{15}H_{16}FN_2O_7S$ $(M\text{-}H)^-$ 387.0668; found 387.0665.

**Radiochemistry.** *General.* [$^{18}$F]Fluoride was produced by the $^{18}O(p,n)^{18}F$ nuclear reaction through proton irradiation of enriched (98%) $^{18}O$ water (3.0 mL, Rotem, Germany) using a TR19/9 cyclotron (Advanced Cyclotron Systems, Inc., Richmond, BC, Canada). Cyclotron-produced [$^{18}$F]fluoride was then trapped on a Waters (Milford, MA, US) Sep-Pak light QMA anion-exchange cartridge (filled with quaternary ammonium chloride polymer) and eluted off with 86% $K_{2.2.2.}/K_2CO_3$ (1.5 mL) and used for radiolabeling of the sulfonium precursor according to Way et al.[18] Semipreparative HPLC purification was completed via the reported procedure. The HPLC purified [$^{18}$F]FIB was diluted with 20 mL of water and trapped on a Phenomenex Strata X (30 mg) cartridge. The solid phase extraction (SPE) cartridge was then washed with additional water (5 mL), and then [$^{18}$F]FIB was eluted off in the appropriate solvent (500 $\mu$L). The stock solution of [$^{18}$F]FIB was used for the optimization experiments.

*Optimization of Radiosynthesis of [$^{18}$F]FB-GSH.* Stock solutions of GSH, [$^{18}$F]FIB, XantPhos Pd G3, and $NEt_3$ in appropriate aqueous and organic solvents were prepared freshly. Aliquots of the stock solutions were added to an Eppendorf LoBind microcentrifuge tube according to each optimization condition. The volume of the reaction mixture was adjusted to 350 $\mu$L to concur with the solvent combinations summarized in Table 1, and the reaction tube was closed. The reaction mixture was allowed to mix on an Eppendorf Thermomixer for 1 min; then, the base was added until the pH was ∼9 (40−60 $\mu$L). The tube was closed and allowed to mix for 15−30 min at 37 °C. After the reaction time, the reaction mixture was diluted with 0.2% TFA/$H_2O$ (1.5 mL) and was injected into the HPLC for analysis (Phenomenex Luna C-18, A = 0.2% TFA/$H_2O$, B= $CH_3CN$. Flow rate: 3 mL/min. Gradient: 0−5 min 20% B, 15 min 50% B, 15−20 min 50% B, 25 min 90% B, 25−35 min 90% B, $t_R$ = 23.1 min).

*Radiosynthesis of [$^{18}$F]FB-LCKLSL.* 0.65 mg (1 $\mu$mol) of LCKLSL was dissolved in 100 $\mu$L of PBS and 50 $\mu$L of [$^{18}$F]FIB (20−30 MBq) in THF, and 50 $\mu$L stock of XantPhos Pd G3 in THF was added to an Eppendorf LoBind microcentrifuge tube.

The reaction tube was closed and was allowed to mix on an Eppendorf Thermomixer for 1 min, and then 50 $\mu$L of $NEt_3$ stock solution in THF was added until the pH was ∼9 (40−60 $\mu$L) followed by 50 $\mu$L of PBS. The tube was closed and allowed to shake for 15 min. After the reaction time, the reaction mixture was diluted with 0.2% TFA/$H_2O$ (1.5 mL) and injected into a semipreparative HPLC to isolate the *S*-arylated compound [$^{18}$F]FB-LCKLSL in 73% radiochemical yield ($t_R$ = 25.1 min). HPLC conditions: (Phenomenex Luna C-18, A = 0.2% TFA/$H_2O$, B = $CH_3CN$. Flow rate: 3 mL/min. Gradient: 0−5 min 20% B, 15 min 50% B, 15−20 min 50% B, 25 min 90% B, 25−35 min 90% B). HPLC coinjection of reference compound FB-LCKLSL confirmed the identity of radiopeptide [$^{18}$F]FB-LCKLSL.

*Radiosynthesis of [$^{18}$F]FB-LYCWHL.* 0.93 mg (1 $\mu$mol) of LYCWHL was dissolved in 100 $\mu$L of PBS and 50 $\mu$L of [$^{18}$F]FIB (20−30 MBq) in THF, and 50 $\mu$L stock of XantPhos Pd G3 in THF was added to an Eppendorf LoBind microcentrifuge tube. The reaction tube was closed and was allowed to mix on an Eppendorf Thermomixer for 1 min, and then 50 $\mu$L of $NEt_3$ stock solution in THF was added until the pH was ∼9 (40−60 $\mu$L) followed by 50 $\mu$L of PBS. The tube was closed and allowed to shake for 15 min at 37 °C. After the reaction time, the reaction mixture was diluted with 0.2% TFA/$H_2O$ (1.5 mL) and injected into a semipreparative HPLC to isolate the *S*-arylated compound [$^{18}$F]FB-LYCWHL in 83% radiochemical yield ($t_R$ = 32.4 min). HPLC conditions: (Phenomenex Luna C-18, A = 0.2% TFA/$H_2O$, B = $CH_3CN$. Flow rate: 3 mL/min. Gradient: 0−5 min 20% B, 15 min 50% B, 15−20 min 50% B, 25 min 90% B, 25−35 min 90% B). HPLC coinjection of reference compound FB-LCKLSL confirmed the identity of radiopeptide [$^{18}$F]FB-LCKLSL.

*Manual Radiosynthesis of [$^{18}$F]6.* 100 $\mu$L of PBS stock solution containing 78 $\mu$g (0.2 $\mu$mol) of compound **5** was added to a mixture of 50 $\mu$L of HPLC-purified [$^{18}$F]FIB (20−30 MBq) in THF and 50 $\mu$L of XantPhos Pd G3 in THF in an Eppendorf LoBind microcentrifuge tube. The reaction tube was closed and was allowed to mix on an Eppendorf Thermomixer for 1 min, and then 50 $\mu$L of PBS and 50 $\mu$L of $NEt_3$ stock solution in $CH_3CN$ was added until the pH was ∼9 (40−60 $\mu$L). The tube was closed and allowed to shake for 15 min at 37 °C. Then, the reaction mixture was diluted with 0.2% TFA/$H_2O$ (1.5 mL) and was injected to the semi-preparative HPLC (Phenomenex Luna 5 mm PFP(2), A = 0.2% TFA/$H_2O$, B = $CH_3CN$. Flow rate: 2 mL/min. Gradient: 0−15 min 5% B, 20 min 10% B, 35−45 min 40% B) to isolate *S*-arylated radioligand [$^{18}$**F**]**6** in 73% radiochemical yield, starting from [$^{18}$F]FIB ($t_R$= 30.5 min). The identity of radioligand [$^{18}$**F**]**6** was confirmed by HPLC analysis via coinjection of reference compound **6**.

*Automated radiosynthesis of [$^{18}$F]6.* Radiosynthesis of [$^{18}$**F**]**6** was performed on a GE TRACERlab FX. The ASU was modified in terms of program and hardware. The synthetic procedure started with the elution of resin-bound cyclotron-produced [$^{18}$F]fluoride from the Waters Sep-Pak light QMA anion-exchange column into reactor 1 of the GE TRACERlab FX using a solution of 86% $K_{2.2.2.}/K_2CO_3$ (1.5 mL). [$^{18}$F]Fluoride was dried azeotropically under vacuum under a steady stream of nitrogen at 50 and 95 °C. To the dried [$^{18}$F]fluoride, (4-iodophenyl)diphenylsulfonium triflate (14 mg) in $CH_3CN$ (1 mL) was added and reacted for 15 min at 90 °C. Once the reaction was completed (15 min), the mixture was diluted with water (12 mL) and passed through a Phenomenex Strata X (30 mg) cartridge. The cartridge was washed with additional water (10 mL), and [$^{18}$F]FIB was eluted off in $CH_3CN$ (500 $\mu$L) into reactor 2 of the ASU, which was charged with 25 $\mu$L of $NEt_3$. 1.5 mg of compound **5** dissolved in PBS (500 $\mu$L) and 0.4 mg of XantPhos Pd G3 dissolved in $CH_3CN$ (200 $\mu$L) were added to reactor 2.

The mixture was allowed to react for 15−30 min at 37 °C. After the reaction time, the mixture was diluted with 1:1 0.2% TFA/$H_2O$:$CH_3CN$ and transferred to the collection vial. The mixture was diluted with 0.2% TFA/$H_2O$ and injected into an HPLC under the conditions described for the manual synthesis. The pure fraction ($t_R$ = 30−32 min) was collected and subjected to evaporation of volatiles *in vacuo*, which usually takes 15−20 min. After the removal of volatiles, radioligand [$^{18}$**F**]**6** was resolubilized in 3 mL of PBS buffer (pH = 7.3, 0.1 mM) for *in vivo* and *in vitro* studies. The isolated decay-corrected radiochemical yield of radioligand


https://doi.org/10.1021/acs.bioconjchem.3c00522
Bioconjugate Chem. 2024, 35, 232−244

[$^{18}$F]**6** was 21 ± 6%, starting from cyclotron-produced [$^{18}$F]fluoride. After HPLC purification, the radiochemical purity exceeded 95%, and the molar activity was ∼40 GBq/μmol. The total synthesis time was 120 min, including HPLC purification and resolubilization.

*Determination ofLipophilicity.* Lipophilicity was determined according to the shake-flask method[21] by measuring the distribution coefficient of radioligand [$^{18}$F]**6** in *n*-octanol and PBS buffer (pH 7.4) as an aqueous phase. The organic and the aqueous phases were presaturated 24 h before the actual start of the experiment. 500 μL of each layer was added to 300−2000 kBq of radioligand [$^{18}$F]**6** in a LoBind Eppendorf tube, and the mixture was shaken intensively for 5 min.

The layers were allowed to separate by centrifugation at 2000 rpm for 2 min. Aliquots of 100 μL were removed from each phase and measured in a gamma counter. Calculated log *D* values are expressed as mean ± SD and summarize three experiments.

*Competitive Binding Assay.* As described before, in vitro competitive binding was analyzed in human prostate adenocarcinoma LNCaP cells in triplicate.[20,22] Briefly, the determination of the concentration of half-maximum inhibition ($IC_{50}$ values) was carried out as a competition against [$^{18}$F]PSMA-1007 using increasing concentrations of PSMA inhibitors 2-PMPA, compound **6**, PSMA-1007 in the range of 0.1 nM to 100 μM. After incubation for 2 h at 37 °C and several washing steps, the cells were harvested. Counts per minute (cpm) of cell-associated radioactivity were measured in a Wizard gamma counter, decay-corrected, and plotted versus log of the PSMA inhibitor concentration to give the typical sigmoidal dose−response curves. All data are presented as means ± SEM from *n* experiments.

**Cell Uptake Experiments.** *Cell Culture.* LNCaP cells obtained from ATCC (cat #CRL-1740) and were grown in RPMI-1640 media (in-house preparation) supplemented with 10% fetal bovine serum (FBS) (Gibco, cat #A7364.01) and 1% penicillin-streptomycin (10,000 mg/mL) (Gibco, cat #15140−122). Cells were incubated at 37 °C in a humidified incubator with a 5% (v/v) $CO_2$ atmosphere (ThermoForma Series II Water Jacketed $CO_2$ Incubator). Cells were grown to confluency in coated T175 flasks (Nunc EasyFlask Nunclon Delta). All coatings were completed using poly-L-lysine solution (PLL) (Sigma, P4707−50 mL) for 1 h at room temperature. Cells were trypsinized with 0.25% Gibco Trypsin-EDTA (cat# 25200−072) for 1−2 min at room temperature. Cells were counted using an automated cell counter (BioRad TC20), and then cells (200k) were plated into 12-well plates (Nunclon Delta, Cat#150628) 72 h before the start of the cell uptake assays.

*Buffer Solutions.* RIPA buffer was prepared in-house and contains the following: Tris-HCl (6.04 g), NaCl (8.76 g), SDS (1 g), sodium deoxycholate (5 g), Triton X-100 (5 mL), and Barnstead water (1 L). Krebs buffer solution was prepared in-house as follows: into Barnstead water (950 mL) was weighed the following: NaCl (7.01 g), $NaHCO_3$ (2.1 g), KCl (0.3 g), $KH_2PO_4$ (0.16 g), $MgSO_4$ (0.3 g), $CaCl_2{\cdot}2H_2O$ (10.3 mg). The solution was then pH adjusted to 7.4 and topped up to 1 L total volume.

*Cell Uptake and Blocking Studies with Radioligand [$^{18}$F]6.* After radiotracer synthesis, the required radioactivity was diluted to dispense 0.4 MBq of radioligand [$^{18}$F]**6** per well in Krebs buffer (300 μL). Once the radiotracer dilution was completed, the starting radioactivity for the assay was recorded on a dose calibrator with the total activity amount and time recorded. Before radiotracer addition to the cells, the growth medium was removed, and the cells were rinsed with room temperature Krebs buffer (2 × 500 μL). Then, the radiotracer solution (300 μL) was added to each well. Plates were incubated at 37 °C for various time points. Upon completion of the time point, the radiotracer was removed, and the wells were rinsed with ice-cold Krebs buffer (2 × 500 μL) to stop the uptake. Once the wells were thoroughly washed, the cells were lysed with RIPA buffer (400 μL) in each well. The RIPA solution was allowed to sit on the cells for a minimum of 10 min. Cell lysates were then removed by scraping and mixing the lysate in the wells. Cell lysate (300 μL) was removed from each well into labeled scintillation vials for gamma counting (Hidex Gamma Counter). All wells of a radiotracer uptake assay were used for protein quantification by the bicinchoninic acid assay (BCA) (Pierce BCA Protein Assay Kit (cat # 23227). Acquired gamma counter data and BCA data were then analyzed to obtain the percentage applied radiotracer per mg protein.

Varying concentrations of PSMA inhibitors DCFPyl (0.1 μM to 1 mM) and compound **6** (1 mM) were prepared in Krebs buffer. Before inhibitor addition to the cells, the growth medium was removed, and the cells were rinsed with room temperature Krebs buffer (2 × 500 μL). DCFPyl or compound **6** (150 μL) was added to each well and allowed to sit for 5 min at room temperature before adding radioligand [$^{18}$F]**6**.

The required radioactivity was diluted to achieve 0.3 MBq of radiolabeled product per well in Krebs buffer (150 μL). Then, the radiotracer solution (150 μL), which already contains DCFPyl or compound **6** as the blocking agent, was added to each well. Plates were incubated at 37 °C for 60 min. Upon completion of the time point, the radiotracer was removed, and the wells were rinsed with ice-cold Krebs buffer (2 × 500 μL) to stop the uptake. Once the wells were thoroughly washed, the cells were lysed with RIPA buffer (400 μL) in each well. The RIPA solution was allowed to sit on the cells for a minimum of 10 min. Cell lysates were then removed by scraping and mixing the lysate in the wells. The cell lysate (300 μL) was removed from each well into labeled scintillation vials for gamma counting. All wells of a radiotracer uptake assay were used for protein quantification by the BCA assay. Acquired gamma counter data and BCA data were then analyzed to obtain the percentage applied radiotracer per mg protein.

**PET Studies.** All animal experiments were performed following the guidelines of the Canadian Council on Animal Care (CCAC) and approved by the local animal care committee (Cross Cancer Institute). Experiments were carried out in LNCaP tumor-bearing BALB/c nude mice (Charles River Laboratories, Quebec, Canada). Male BALB/c nude mice were housed under standard conditions with free access to regular food and tap water.

Around 20 × $10^6$ LNCaP cells in 200 μL of PBS/Matrigel 50/50) were injected into the upper left flank of these mice (20−24 g, 4−6 months of age). One day prior to the LNCaP cell injection, mice were also implanted with a 1.5 mg/pellet containing dehydroepiandrosterone (DHEA) in a 60-day release preparation (Innovative Research of America, Sarasota, FL, U.S.A.) subcutaneously into the right flank. After approximately 5−7 weeks, LNCaP tumors reached ∼400−500 $mm^3$ and were used for PET experiments.


https://doi.org/10.1021/acs.bioconjchem.3c00522
Bioconjugate Chem. 2024, 35, 232−244

**Dynamic PET Experiments.** General anesthesia of tumor-bearing mice was induced with 4−5% isoflurane and maintained during the study with 1.5% isoflurane in 40% oxygen/60% nitrogen (gas flow 1 mL/min). The body temperature was kept constant at 37 °C for the entire experiment. Mice were positioned in a prone position into the center field of view of an INVEON PET/CT scanner (Siemens Preclinical Solutions, Knoxville, TN, USA). A transmission scan for attenuation correction was not acquired. Mice were injected with 6−8 MBq of radioligand [$^{18}$F]**6** in 100−150 $\mu$L of saline (0.9% NaCl) through a tail vein catheter. For blocking studies, animals were predosed with 300 $\mu$g of DCFPyL and compound **6** in 50 $\mu$L of saline about 5 min before radiotracer injection. Data acquisition was performed dynamically over 60 min in a 3D list mode. Dynamic list mode data were sorted into sinograms with 54-time frames (10 × 2, 8 × 5, 6 × 10, 6 × 20, 8 × 60, 10 × 120, 6 × 300 s). The frames were reconstructed using maximum a posteriori (MAP). The pixel size was 0.085 by 0.085 by 0.121 mm3 (256 × 256 × 63), and the resolution in the center of the field of view was ∼1.8 mm. No correction for partial volume effects was applied. The image files were further processed using ROVER v2.0.51 software (ABX GmbH, Radeberg, Germany). Masks defining 3D regions of interest (ROI) were drawn, and the ROIs were defined by a thresholding of 50%. Mean standardized uptake values (SUVmean = (activity/mL tissue)/(injected activity/body weight), mL/g) were calculated for each ROI. Time−activity curves (TAC) were generated from defined ROIs using GraphPad Prism 5.0 (GraphPad Software, San Diego, CA). All semiquantified PET data are presented as means ± SEM from $n$ experiments. Statistical differences were tested by unpaired Student's $t$-test and considered significant for $p < 0.05$.

## ■ ASSOCIATED CONTENT

### Supporting Information

The Supporting Information is available free of charge at https://pubs.acs.org/doi/10.1021/acs.bioconjchem.3c00522.

HPLC traces and NMR spectra of all compounds prepared in the manuscript (PDF)

## ■ AUTHOR INFORMATION


### Corresponding Author

**Frank Wuest** − *Department of Chemistry, University of Alberta, Edmonton, Alberta T6G 2G2, Canada; Department of Oncology, University of Alberta, Cross Cancer Institute, Edmonton, Alberta T6G 2 × 4, Canada; Cancer Research Institute of Northern Alberta, University of Alberta, Edmonton, AB T6G 2E1, Canada;* orcid.org/0000-0002-6705-6450; Email: wuest@ualberta.ca

### Authors

**Felix Francis** − *Department of Chemistry, University of Alberta, Edmonton, Alberta T6G 2G2, Canada*

**Melinda Wuest** − *Department of Oncology, University of Alberta, Cross Cancer Institute, Edmonton, Alberta T6G 2 × 4, Canada; Cancer Research Institute of Northern Alberta, University of Alberta, Edmonton, AB T6G 2E1, Canada*

**Jenilee D. Woodfield** − *Department of Oncology, University of Alberta, Cross Cancer Institute, Edmonton, Alberta T6G 2 × 4, Canada*

Complete contact information is available at: https://pubs.acs.org/10.1021/acs.bioconjchem.3c00522


### Notes

The authors declare no competing financial interest.

## ■ ACKNOWLEDGMENTS

The authors thank the Edmonton PET Centre for radionuclide production and Angela Westover and Jeff Mcpherson for providing [$^{18}$F]PSMA-1007. We also thank Jennifer Dufour for her help with the cell cuptake experiments. F.W. thanks the Dianne and Irving Kipnes Foundation for supporting this work.

## ■ REFERENCES


(1) Rodríguez, J.; Martínez-Calvo, M. Transition-Metal-Mediated Modification of Biomolecules. *Chemistry.* **2020**, *26* (44), 9792−9813.

(2) Jbara, M.; Maity, S. K.; Brik, A. Palladium in the Chemical Synthesis and Modification of Proteins. *Angew. Chem., Int. Ed. Engl.* **2017**, *56* (36), 10644−10655.

(3) Vinogradova, E. V.; Zhang, C.; Spokoyny, A. M.; Pentelute, B. L.; Buchwald, S. L. Organometallic palladium reagents for cysteine bioconjugation. *Nature.* **2015**, *526* (7575), 687−691.

(4) Zhang, C.; Vinogradova, E. V.; Spokoyny, A. M.; Buchwald, S. L.; Pentelute, B. L. Arylation Chemistry for Bioconjugation. *Angew. Chem., Int. Ed. Engl.* **2019**, *58* (15), 4810−4839.

(5) Cal, P. M.; Bernardes, G. J.; Gois, P. M. Cysteine-selective reactions for antibody conjugation. *Angew. Chem., Int. Ed. Engl.* **2014**, *53* (40), 10585−10587.

(6) Chalker, J. M.; Bernardes, G. J.; Lin, Y. A.; Davis, B. G. Chemical modification of proteins at cysteine: opportunities in chemistry and biology. *Chem. Asian J.* **2009**, *4* (5), 630−640.

(7) Rojas, A. J.; Pentelute, B. L.; Buchwald, S. L. Water-Soluble Palladium Reagents for Cysteine S-Arylation under Ambient Aqueous Conditions. *Org. Lett.* **2017**, *19* (16), 4263−4266.

(8) Al-Shuaeeb, R. A.; Kolodych, S.; Koniev, O.; Delacroix, S.; Erb, S.; Nicolaÿ, S.; Cintrat, J. C.; Brion, J. D.; Cianférani, S.; Alami, M.; Wagner, A.; Messaoudi, S. Palladium-Catalyzed Chemoselective and Biocompatible Functionalization of Cysteine-Containing Molecules at Room Temperature. *Chemistry.* **2016**, *22* (32), 11365−11370.

(9) Humpert, S.; Omrane, M. A.; Urusova, E. A.; Gremer, L.; Willbold, D.; Endepols, H.; Krasikova, R. N.; Neumaier, B.; Zlatopolskiy, B. D. Rapid 18F-labeling via Pd-catalyzed S-arylation in aqueous medium. *Chem. Commun. (Camb).* **2021**, *57* (29), 3547−3550.

(10) McDaniel, J. W.; Stauber, J. M.; Doud, E. A.; Spokoyny, A. M.; Murphy, J. M. An Organometallic Gold(III) Reagent for 18F Labeling of Unprotected Peptides and Sugars in Aqueous Media. *Org. Lett.* **2022**, *24* (28), 5132−5136.

(11) Way, J.; Bouvet, V.; Wuest, F. Synthesis of 4-[18F]-fluorohalobenzenes and palladium-mediated cross-coupling reactions for the synthesis of 18F-labled radiotracers. *Curr. Org. Chem.* **2013**, *17*, 2138−2152.

(12) Alonso Martinez, L. M.; DaSilva, J. N. Development of a novel [18 F]fluorobenzyl derivative of the AT1 receptor antagonist Candesartan. *J. Labelled Comp Radiopharm.* **2021**, *64* (3), 120−128.

(13) Kügler, F.; Ermert, J.; Kaufholz, P.; Coenen, H. H. 4-[18F]Fluorophenylpiperazines by improved Hartwig-Buchwald N-arylation of 4-[18F]fluoroiodobenzene, formed via hypervalent λ3-iodane precursors: application to build-up of the dopamine D4 ligand [18F]FAUC 316. *Molecules.* **2015**, *20* (1), 470−486.

(14) Yagi, Y.; Kimura, H.; Arimitsu, K.; Ono, M.; Maeda, K.; Kusuhara, H.; Kajimoto, T.; Sugiyama, Y.; Saji, H. The synthesis of [18F]pitavastatin as a tracer for hOATP using the Suzuki coupling. *Org. Biomol Chem.* **2015**, *13* (4), 1113−1121.

(15) Brooks, A. F.; Topczewski, J. J.; Ichiishi, N.; Sanford, M. S.; Scott, P. J. Late-stage [18F]Fluorination: New Solutions to Old Problems. *Chem. Sci.* **2014**, *5* (12), 4545−4553.

(16) Cole, E. L.; Stewart, M. N.; Littich, R.; Hoareau, R.; Scott, P. J. Radiosyntheses using fluorine-18: the art and science of late stage fluorination. *Curr. Top Med. Chem.* **2014**, *14* (7), 875−900.

(17) Brooks, A. F.; Topczewski, J. J.; Ichiishi, N.; Sanford, M. S.; Scott, P. J. H. Late-stage [18F]Fluorination: New Solutions to Old Problems. *Chem. Sci.* **2014**, *5* (12), 4545−4553.
(18) Way, J. D.; Wuest, F. Automated radiosynthesis of no-carrier-added 4-[18F]fluoroiodobenzene: a versatile building block in 18F radiochemistry. *J. Labelled Comp Radiopharm.* **2014**, *57* (2), 104−109.
(19) Bruno, N. C.; Tudge, M. T.; Buchwald, S. L. Design and Preparation of New Palladium Precatalysts for C-C and C-N Cross-Coupling Reactions. *Chem. Sci.* **2013**, *4*, 916−920.
(20) Gade, N. R.; Kaur, J.; Bhardwaj, A.; Ebrahimi, E.; Dufour, J.; Wuest, M.; Wuest, F. N-Alkyl Carbamoylimidazoles as Versatile Synthons for the Synthesis of Urea-Based PSMA Inhibitors. *ACS Med. Chem. Lett.* **2023**, *14* (7), 943−948.
(21) Waterhouse, R. N. Determination of lipophilicity and its use as a predictor of blood-brain barrier penetration of molecular imaging agents. *Mol. Imaging Biol.* **2003**, *5* (6), 376−389.
(22) Bouvet, V.; Wuest, M.; Bailey, J. J.; Bergman, C.; Janzen, N.; Valliant, J. F.; Wuest, F. Targeting Prostate-Specific Membrane Antigen (PSMA) with F-18-Labeled Compounds: the Influence of Prosthetic Groups on Tumor Uptake and Clearance Profile. *Mol. Imaging Biol.* **2017**, *19* (6), 923−932.
(23) Bernard-Gauthier, V.; Lepage, M. L.; Waengler, B.; Bailey, J. J.; Liang, S. H.; Perrin, D. M.; Vasdev, N.; Schirrmacher, R. Recent Advances in 18F Radiochemistry: A Focus on B-18F, Si-18F, Al-18F, and C-18F Radiofluorination via Spirocyclic Iodonium Ylides. *J. Nucl. Med.* **2018**, *59* (4), 568−572.
(24) Capasso, G.; Stefanucci, A.; Tolomeo, A. A systematic review on the current status of PSMA-targeted imaging and radioligand therapy. *Eur. J. Med. Chem.* **2024**, *263*, No. 115966.
(25) Mease, R. C.; Dusich, C. L.; Foss, C. A.; Ravert, H. T.; Dannals, R. F.; Seidel, J.; Prideaux, A.; Fox, J. J.; Sgouros, G.; Kozikowski, A. P.; Pomper, M. G. N-[N-[(S)-1,3-Dicarboxy-propyl]carbamoyl]-4-[18F]-fluorobenzyl-L-cysteine, [18F]DCFBC: a new imaging probe for prostate cancer. *Clin. Cancer Res.* **2008**, *14* (10), 3036−3043.
(26) Fallah, J.; Agrawal, S.; Gittleman, H.; Fiero, M. H.; Subramaniam, S.; John, C.; Chen, W.; Ricks, T. K.; Niu, G.; Fotenos, A.; Wang, M.; Chiang, K.; Pierce, W. F.; Suzman, D. L.; Tang, S.; Pazdur, R.; Amiri-Kordestani, L.; Ibrahim, A.; Kluetz, P. G. FDA Approval Summary: Lutetium Lu 177 Vipivotide Tetraxetan for Patients with Metastatic Castration-Resistant Prostate Cancer. *Clin. Cancer Res.* **2023**, *29* (9), 1651−1657.
(27) Lucaroni, L.; Georgiev, T.; Prodi, E.; Puglioli, S.; Pellegrino, C.; Favalli, N.; Prati, L.; Manz, M. G.; Cazzamalli, S.; Neri, D.; Oehler, S.; Bassi, G. Cross-reactivity to glutamate carboxypeptidase III causes undesired salivary gland and kidney uptake of PSMA-targeted small-molecule radionuclide therapeutics. *Eur. J. Nucl. Med. Mol. Imaging.* **2023**, *50* (3), 957−961.
(28) Huang, S. S.; DiFilippo, F.; Lindner, D.; Heston, W. D. W. Intriguing information from recent letter and article regarding unwanted targeting of salivary glands by PSMA ligands. *Eur. J. Nucl. Med. Mol. Imaging.* **2023**, *50* (10), 2950−2951.
(29) Lee, Z.; Heston, W. D.; Wang, X.; Basilion, J. P. GCP III is not the ″off-target″ for urea-based PSMA ligands. *Eur. J. Nucl. Med. Mol. Imaging.* **2023**, *50* (10), 2944−2946.
(30) Sharma, S. K.; Al-Hourani, B. J.; Wuest, M.; Mane, J. Y.; Tuszynski, J.; Baracos, V.; Suresh, M.; Wuest, F. Synthesis and evaluation of fluorobenzoylated di- and tripeptides as inhibitors of cyclooxygenase-2 (COX-2). *Bioorg. Med. Chem.* **2012**, *20* (7), 2221−2226.
(31) Wuest, M.; Perreault, A.; Kapty, J.; Richter, S.; Foerster, C.; Bergman, C.; Way, J.; Mercer, J.; Wuest, F. Radiopharmacological evaluation of (18)F-labeled phosphatidylserine-binding peptides for molecular imaging of apoptosis. *Nucl. Med. Biol.* **2015**, *42* (11), 864−874.


https://doi.org/10.1021/acs.bioconjchem.3c00522
*Bioconjugate Chem.* 2024, 35, 232−244